Human Papillomavirus Types 16, 18, and 31 Share Similar Endocytic Requirements for Entry

Gilles Spoden,[a] Lena Kühling,[b] Nicole Cordes,[b] Bettina Frenzel,[a] Martin Sapp,[c] Klaus Boller,[d] Luise Florin,[a] Mario Schelhaas[b]

Department of Medical Microbiology and Hygiene, University Medical Centre of the Johannes Gutenberg University, Mainz, Germany[a]; Emmy-Noether Group Virus Endocytosis, Institutes of Molecular Virology and Medical Biochemistry, University of Münster, Münster, Germany[b]; Department of Microbiology and Immunology, Feist-Weiller Cancer Center, Center for Molecular Tumor Virology, LSU Health Sciences Center, Shreveport, Louisiana, USA[c]; Paul Ehrlich Institute, Langen, Germany[d]

Human papillomavirus type 18 (HPV18), one of the HPVs with malignant potential, enters cells by an unknown endocytic mechanism. The key cellular requirements for HPV18 endocytosis were tested in comparison to those for HPV16 and -31 endocytoses. HPV18 (like HPV16 and -31) entry was independent of clathrin, caveolin, dynamin, and lipid rafts but required actin polymerization and tetraspanin CD151, and the viruses were routed to the same LAMP-1-positive compartment. Hence, the viruses shared similar cellular requirements for endocytic entry.

The human papillomaviruses (HPVs) are a family of nonenveloped DNA viruses with transforming potential. A particular subgroup of HPVs, the high-risk types, are additionally associated with cervical and anogenital cancers. Of those high-risk types, HPV type 16 (HPV16) is the most prevalent and the best studied. HPVs enter the basal cells of squamous epithelia by endocytosis during initial infection (1). For cell entry, most viruses employ one of several existing pathways for endocytosis (2, 3). These pathways are typically differentiated by the cellular proteins mediating endocytic vacuole formation, by the ultrastructural morphology of endocytic pits, and by the timing of vesicle formation (2–4). Although HPV16 cell entry was originally attributed to clathrin-mediated endocytosis (CME) in various cell types (5–8), it has recently been shown that HPV16 enters cells by a novel ligand-induced endocytic pathway that is clathrin, caveolin, lipid raft, and dynamin independent but that depends on highly regulated actin dynamics and an association with CD151-containing tetraspanin-enriched microdomains (9–11) The high-risk-type HPV31 may differ in the mode of endocytosis from HPV16, as it has been described to enter into human keratinocytes by a caveolin/lipid raft-mediated mechanism (12). However, in COS-7 cells and 293TT cells, HPV16 and -31 endocytoses appear to occur by a similar mechanism that is independent of lipid rafts (5).

One of the more-prevalent high-risk types, which has not been analyzed for its mode of endocytic entry, is HPV18. Here, we aimed to delineate the general endocytic requirements for infectious HPV18 endocytosis. In particular, we aimed to analyze whether HPV18 exhibits requirements similar to those of HPV16 or -31 for endocytic entry into host cells. Therefore, we compared the efficacy of cell entry after cell perturbation for the main determinants of several endocytic pathways in HeLa and HaCaT cells. The cell biological determinants that allow differentiation of the different endocytic pathways include clathrin for CME, caveolin for caveolin-mediated mechanisms, cholesterol depletion for lipid raft-dependent mechanisms (e.g., caveolar/lipid raft endocytosis or glycosphingolipid-enriched endocytic carriers), dynamin-2 for dynamin-mediated endocytic processes (e.g., CME, caveolar endocytosis, and the interleukin-2 pathway), and actin polymerization dynamics for actin-mediated endocytic processes (macropinocytosis, caveolar endocytosis, and HPV16 endocytosis) (summarized in references 3 and 4). For perturbation of these

determinants, RNA interference (RNAi)-mediated knockdown of cellular factors, small-compound inhibitors, and the expression of dominant-negative (DN) proteins were used. To follow HPV entry, we employed the pseudovirion (PsV) system. This system makes use of a viral pseudogenome that encodes a reporter gene that is encapsidated by the major and minor capsid proteins, L1 and L2, respectively (13). The expression of the reporter is used as the readout for successful cell entry after delivery of the viral pseudogenome to the nucleus. Luciferase was used as the reporter in this study, and PsVs were prepared as described previously (14, 15).

HPV16, -18, and -31 PsV preparations yielded homogeneous particles that were about 50 nm in diameter (Fig. 1A). The incorporation of L2 into virions and correct allocation of the capsid proteins were tested using type-specific antibodies for L1 and L2 and Western blotting. For L1 detection, the following antibodies were used: 16L1-212C detecting HPV16 and -31 L1, 312F detecting HPV16 L1 (16), and 18L1-1E detecting HPV18. For L2, L2-1 detecting HPV16 and -31 L2 (17), K18 detecting HPV16 L2 (18), and 18L2-412F detecting HPV18 L2 were used. The mouse monoclonal antibodies 16L1-212C, 18L1-1E, and 18L2-412F were obtained after immunization of BALB/c mice with G16L1-46/269, G18L1 (19), and G18L2 (18) glutathione S-transferase (GST) fusion proteins, respectively, as described previously (17, 19). 16L1-312F, 18L1-1E, and 18L2-412F are type specific for their respective types. 16L2-212C recognizes L1 proteins of the alpha-papillomavirus species 9 HPV types. In all cases, the incorporation of type-specific L2 was detected (Fig. 1B).

HPV entry is asynchronous and slow, with half times of internalization ranging from 4 to 12 h (6, 9, 20–22). To ascertain that the entry of the three HPV types would be evaluated at the same time of progress during entry, we analyzed the kinetics of infection
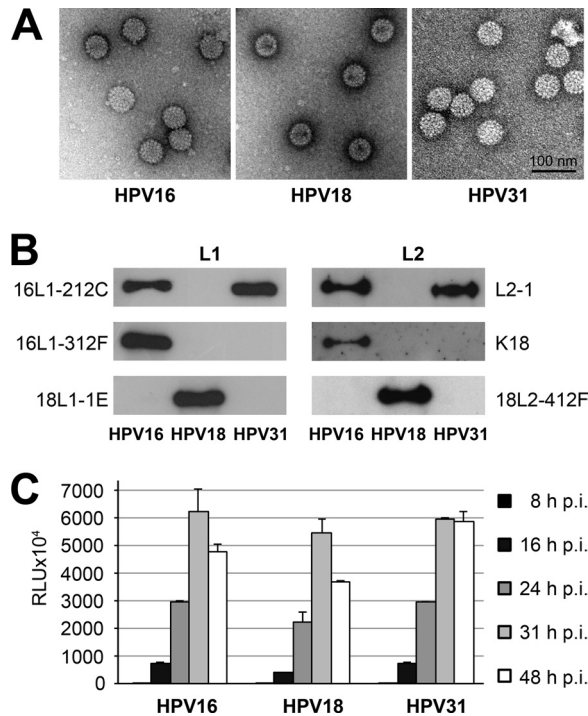
FIG 1 HPV pseudovirion assembly and infection. (A) Purified HPV16, -18, and -31 PsVs were subjected to negative staining and visualized by electron microscopy. (B) HPV PsVs were subjected to SDS-PAGE and analyzed by Western blotting with type-specific L1 antibodies 16L1-212C, 16L1-312F, and 18L1-1E and L2 antibodies L2-1, K18, and 18L2-412F. (C) HeLa cells were infected with HPV16, -18, or -31 PsVs harboring a luciferase reporter. The amounts of luciferase activity were determined at the indicated time points p.i., and background activity of noninfected control cells was subtracted. Activities are given as relative light units (RLU) ± standard deviations (SD).

in HeLa cells. For this, we used PsVs bearing the sensitive luciferase reporter. Luciferase expression was quantified after infection of cells with 1,000 PsVs/cell using the luciferase cell culture lysis reagent and assay system (Promega) as described previously (23). At 16 h postinfection (p.i.), luciferase activity was clearly detectable for all three HPV types (Fig. 1C). Thereafter, luciferase activity increased to reach its maximum at 31 h p.i. (Fig. 1C). As no significant differences between the HPV types were observed, the different HPV types appeared to follow a similar itinerary during cell entry and to enter cells with similar efficiency. In the experiments described hereinafter, infections were quantified at 24 h p.i., when the increase of luciferase expression was linear, so that absolute and kinetic effects of perturbations with respect to infection could be detected.

To analyze whether HPV18, like HPV16 and -31, would enter cells independently of clathrin, we refrained from using the inhibitor chlorpromazine, which is often used for this purpose. Chlorpromazine is supposed to sequester the clathrin adaptor AP2 from membranes (24). However, chlorpromazine can also interfere with the formation of phagosomes or macropinosomes, cause inhibition of phospholipase C (PLC)-regulated actin rearrangements, and change plasma membrane fluidity (25–28). Instead of using chlorpromazine, we initially made use of the DN mutants of Eps15 to block CME. Eps15, which interacts with the major clathrin adaptor protein AP2, is an integral component of clathrin-coated pits, and the expression of the Eps15 DIII or EΔ95/295

mutant inhibits CME (29). To control for the efficacy of inhibition by the dominant-negative constructs, we infected the Eps15-over-expressing cells with Semliki Forrest virus (SFV), which is established as using CME for entry (30). When expressed in HeLa cells, the mutants inhibited SFV but not HPV18 infection compared to the results using the control construct, Eps15 D3Δ2, which does not perturb CME (Fig. 2A and B). As expected, HPV16 and -31 were also not inhibited (Fig. 2A). Instead, we observed an increase of luciferase activity, which may suggest an increased routing of particles into an infectious pathway if CME is blocked. To assess any role of clathrin more directly, clathrin heavy chain (CHC) was depleted from HeLa and HaCaT cells by RNAi after the transfection of 100 nM small interfering RNA (siRNA) oligonucleotides (Hs_CLTC_10; Qiagen) with RNAiMax (Invitrogen). Cells were infected with HPV18 or, as control, with HPV16 or -31 PsVs at 48 h posttransfection. Neither HPV18 nor HPV16 or -31 exhibited any decrease of infection in either HeLa or HaCaT cells, suggesting that clathrin depletion did not inhibit infectious endocytosis (Fig. 2D and E). Instead, luciferase activity was increased in clathrin-depleted cells compared to the level in cells treated with a scrambled siRNA control (AllStars negative-control siRNA; Qiagen). To control the efficiency of knockdown, the abundance of clathrin heavy chain was analyzed by Western blotting using a mouse monoclonal antibody against CHC (clone 23; BD Biosciences). The clathrin level was reduced by about 90% compared to the level in control-transfected cells (Fig. 2C). To assess whether the knockdown levels would functionally perturb CME, we used infection of knockdown cells by SFV and vesicular stomatitis virus (VSV) as controls. Both viruses are established as using CME for entry (30, 31). For quantification by flow cytometry, a recombinant VSV that expresses green fluorescent protein (GFP) was used (9). For SFV, infection was quantified after antibody staining as previously described (9). As expected, RNAi-mediated clathrin depletion significantly inhibited SFV and VSV infection of HeLa cells (Fig. 2F), which suggested that the knockdown was functionally efficient. Taken together, the data indicated that HPV18 infection, similar to HPV16 and -31 infection, does not depend on CME for entry into host cells.

Next, we analyzed whether the caveolin/lipid raft-dependent endocytic mechanism was required for HPV18 infection. Similar to the experiments described above, we infected HeLa and HaCaT cells after RNAi-mediated depletion of caveolin. Cells were transfected with caveolin-1-specific siRNA (Hs_Cav1_6; Qiagen) or the scrambled control for 48 h, followed by infection with HPV18 and with HPV16 and -31 as controls. HPV18 infection was not inhibited by caveolin-1 depletion (Fig. 3A and B). In line with previous reports (9, 10), we also did not observe an inhibition of HPV16 infection (Fig. 3A and B). In addition, we did not observe any inhibitory effect of caveolin-1 knockdown on HPV31 infection. Again, the efficiency of knockdown of caveolin-1 was controlled by Western blotting using a rabbit polyclonal antibody against caveolin-1 (ab18199; Abcam) (Fig. 3I, top). To corroborate our findings, we investigated HPV infection in mouse embryonic fibroblasts (MEFs) from caveolin-1 knockout mice (Fig. 3I, bottom, note the absence of caveolin-1 signal in the Western blot) (32). The luciferase activity after infection with HPV18, as well as after HPV16 and -31 infection of caveolin-1 knockout MEFs, was significantly increased compared to the luciferase activity after infection of wild-type MEFs (Fig. 3C). Altogether, these results suggested that all three HPV types can infect cells independently of
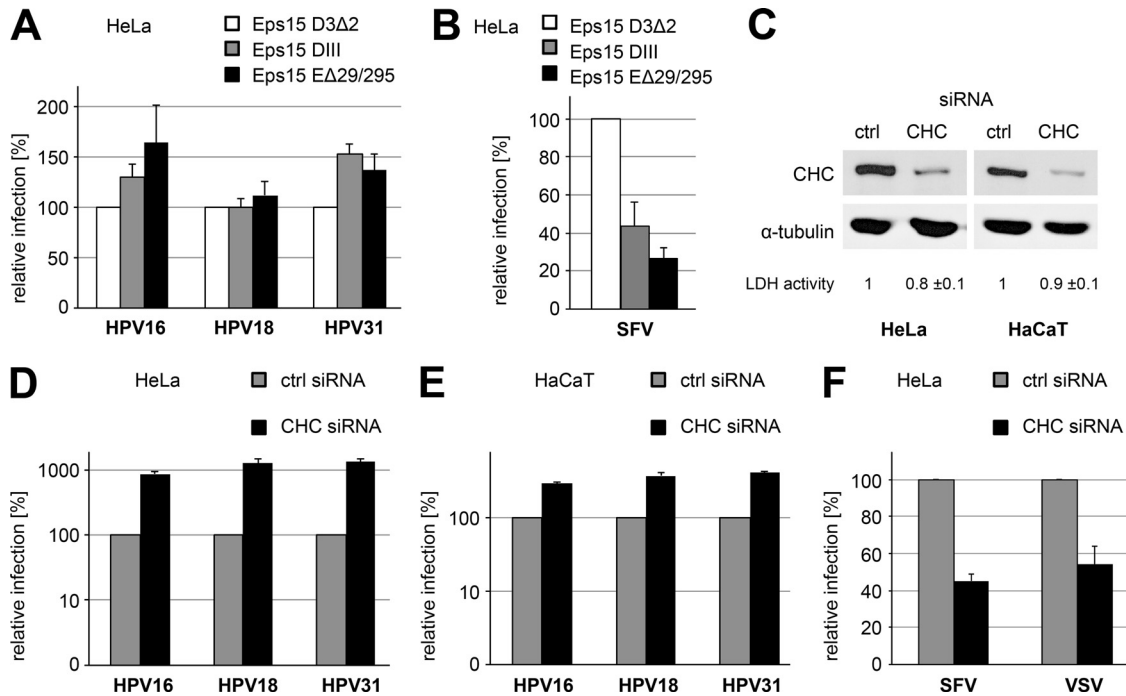
FIG 2 Perturbation of clathrin-mediated endocytosis does not inhibit HPV entry. (A) HeLa cells were transfected for 24 h with the dominant-negative Eps15 mutants DIII and EΔ29/295 or, as a control, with the nonperturbing Eps15 D3Δ2 construct. Cells were subsequently infected with HPV PsVs for 24 h, at which time luciferase activities were measured. Depicted are the amounts of infection (±SD) relative to that in the Eps15 D3Δ2 control cells. (B) The experiment was performed as described for panel A, but cells were infected for 6 h with SFV. Infection by SFV was analyzed by antibody staining using flow cytometry. Given are the amounts of infection (±SD) relative to that in the Eps15 D3Δ2 control cells. (C) HeLa or HaCaT cells were transfected with siRNA targeted against clathrin heavy chain (CHC) or control (ctrl) for 48 h. Cell lysates were analyzed by Western blotting for the levels of CHC or of α-tubulin as a loading control. Also given are lactate dehydrogenase (LDH) activities (±SD) after siRNA transfection relative to that in control-transfected cells, which were used for normalization of the luciferase activities shown in panels D and E. (D, E) siRNA-transfected HeLa or HaCaT cells were infected 48 h after siRNA transfection with HPV PsVs as indicated. At 24 h p.i., luciferase activities were determined. Luciferase activities were normalized to LDH activity for cell viability and are depicted as percentages of infection (±SD) relative to that in control siRNA-transfected cells. (F) siRNA transfection was performed as described for panel D, but cells were infected for 6 h with SFV and VSV as indicated. Infection by SFV or by VSV was analyzed by antibody staining or GFP expression, respectively, using flow cytometry. Given are the amounts of infection (±SD) relative to those in control siRNA-transfected cells.

caveolin. This conclusion is in line with previous observations for HPV16 (9, 10). In contrast, a previous study reports sensitivity of HPV31 to overexpression of GFP–caveolin-1, which has also been dubbed a DN mutant (12). Since the overexpression of caveolin results in the generation of modified endosomal vacuoles (33) and since HPV31 requires endosomal trafficking (34), it is not unlikely that intracellular trafficking of HPV31 was perturbed during entry in GFP–caveolin-1-expressing cells and that this is what caused the reduced infectivity observed by Smith and colleagues (12). Hence, caveolin-1 depletion would not affect the infection of HPV31.

To test whether lipid rafts would be required for HPV18 infection, we depleted HeLa and HaCaT cells of cholesterol by nystatin-progesterone treatment at the concentrations indicated in Figure 3. This combination of drugs is widely used to deplete cholesterol and to inhibit its synthesis (35). Here, cells were treated for 24 h prior to infection, and the treatment was continued throughout infection. As controls, Simian virus 40 (SV40), which requires lipid raft-dependent mechanisms for uptake (32), and SFV, which requires cholesterol in the viral envelope for fusion (36), were used. Both viruses exhibited significantly reduced infection after nystatin-progesterone treatment of HeLa cells (Fig. 3F). In contrast, neither HPV18 nor HPV16 or -31 was inhibited by the cholesterol depletion induced by nystatin-progesterone (Fig. 3D and

E). Also, an alternate inhibitor of lipid rafts, filipin III, did not affect the infectivity of HPV18, -16, or -31 (Fig. 3G and H), which indicated that all three HPV types could enter cells independently of lipid raft-mediated mechanisms of endocytosis.

Next, we analyzed the impact of dynamin-2 on HPV18 infection, as this large GTPase is involved in endocytic vesicle formation for a number of pathways (reviewed in reference 4). For this, we transfected HeLa cells with a GFP-tagged DN mutant of dynamin-2 (K44A) that is deficient in GTP hydrolysis, and we compared the infectivities of HPV18, -16, and -31 in those cells with their infectivities in GFP-transfected control cells. For all HPV types, there was no difference in infectivities between the K44A mutant and the control-expressing cells (Fig. 4A). In contrast, the levels of infection by SFV and SV40, which enter cells by CME and caveolar endocytosis, respectively, were reduced (Fig. 4B) (32, 36). In addition, HeLa and HaCaT were depleted of dynamin-2 by transfection of dynamin-2-specific siRNA (CCGAAUCAAUCGCAUCUUCdTdT; Sigma-Aldrich) (37) for 48 h, resulting in almost complete depletion as judged by Western blotting (Fig. 4E). When infection of HPV18, -16, or -31 was compared to that in control siRNA-transfected cells, no significant difference was observed (Fig. 4C and D). Altogether, our observations suggested that neither HPV18 nor HPV16 or -31 required a dynamin-2-mediated mechanism for endocytosis.
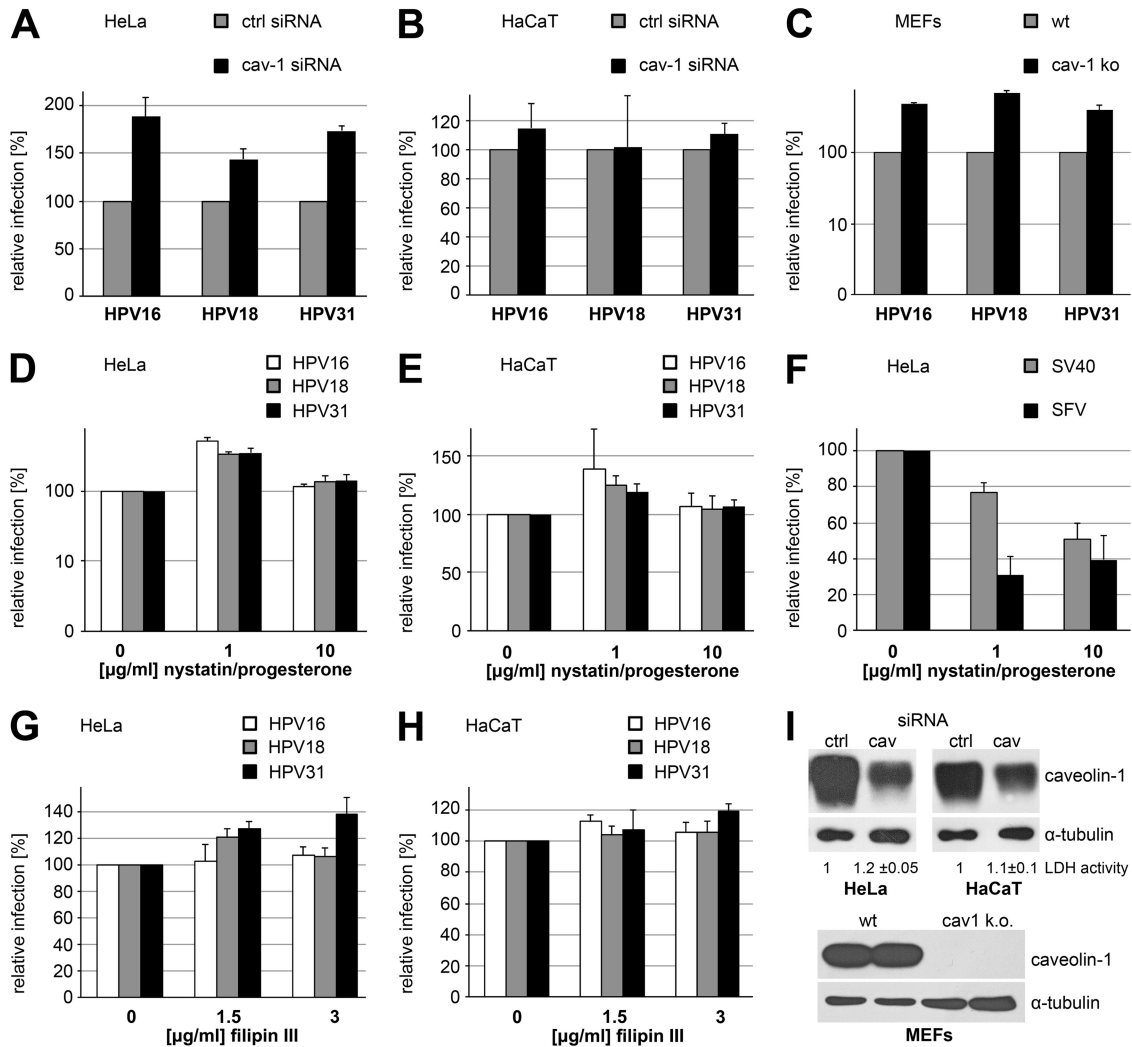
FIG 3 HPV entry is caveolin-1 and lipid raft independent. (A, B) HeLa or HaCaT cells were siRNA transfected with a caveolin-1-specific siRNA or control as described in the legend to Figure 2 and subsequently infected with HPV PsVs as indicated. Infectivities were determined as described in the legend to Figure 2C. (C) Equal cell numbers of wild-type (wt) and caveolin-1 knockout mouse embryonic fibroblasts (MEFs) were infected with HPV PsVs. At 24 h p.i., luciferase activities were determined. Luciferase activities were normalized by an ATP-based cell viability assay (CellTiter-Glo; Promega) and to luciferase activities in control siRNA-transfected cells and are depicted as relative percentages of infection ± SD. (D, E) HeLa or HaCaT cells were preincubated overnight with the indicated concentrations of nystatin-progesterone and subsequently infected with HPV PsVs. At 24 h p.i., luciferase activities were determined. Luciferase activities were normalized to LDH activity for cell viability and are depicted as percentages of infection (±SD) relative to the luciferase activity in dimethyl sulfoxide (DMSO)-treated cells. (F) The experiment was performed as described for panel D, but cells were infected with SV40 or SFV for 24 h or 6 h, respectively. Infection by SV40 or SFV was analyzed by antibody staining against T-antigen or glycoproteins, respectively, using flow cytometry. Given are the amounts of infection (±SD) relative to those in DMSO-treated cells. (G, H) HeLa or HaCaT cells were preincubated with the indicated concentrations of filipin III and infected with HPV PsVs for 24 h. Infectivities were assessed as described for panels D and E. (I) Cell lysates of HeLa or HaCaT cells transfected with caveolin-1 or control siRNA for 48 h (top) or of caveolin wt or knockout (k.o.) MEFs (bottom) were analyzed for the levels of caveolin-1 or, as a loading control, α-tubulin (B-5-1-2; Sigma-Aldrich) by Western blotting. Also depicted are the LDH activities (±SD) after siRNA transfection relative to that in control-transfected cells, which were used for normalization in the experiments whose results are shown in panels A and B.

Since HPV18, as well as HPV16 and -31, was not inhibited by the perturbation of clathrin-, caveolin/lipid raft-, or dynamin-2-mediated mechanisms of endocytosis, we analyzed further factors that have been implicated in HPV16 endocytosis. Among those, regulated actin polymerization and depolymerization contribute to scission of endocytic vesicles during HPV16 uptake (9). To analyze whether actin dynamics are also involved in HPV18 infection, HeLa and HaCaT cells were preincubated with cytochalasin D for 30 min at the concentrations indicated in Figure 5 and were subsequently infected with HPV18, -16, and -31. Like HPV16 and

-31 infection, HPV18 infection was strongly decreased by actin perturbation (Fig. 5A and B). In contrast, SFV infection of HeLa cells was unaffected, and VSV infection was decreased in a concentration-dependent manner as previously reported (Fig. 5C) (9, 38). These results suggested that HPV18 and -31 required actin polymerization for infectious endocytosis, as previously observed for HPV16 and -33 (9, 21).

In addition to actin, CD151, a component of tetraspanin-enriched microdomains, previously shown to be required for HPV16 infection (10, 11), may be involved in HPV18 and -31
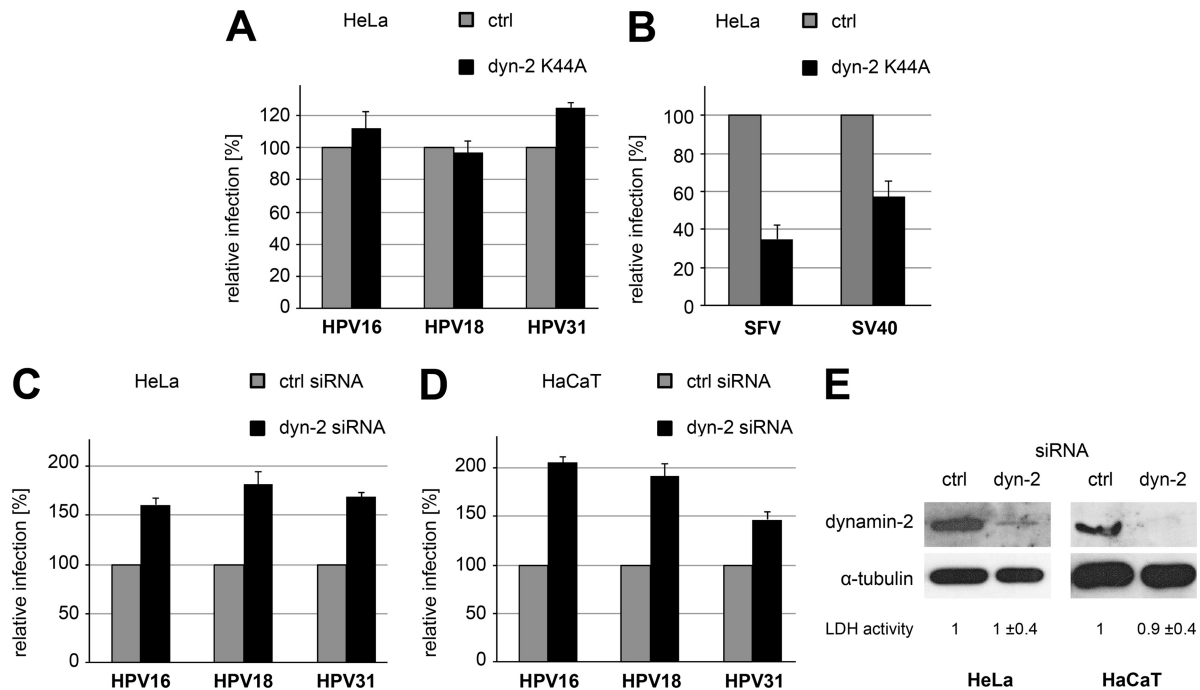
FIG 4 HPV infection is dynamin independent. (A) HeLa cells were transfected for 24 h with constructs expressing GFP or a dominant-negative dynamin-2 (K44A) tagged with GFP and subsequently infected with HPV PsVs. At 24 h p.i., luciferase activities were determined. Luciferase activities were normalized to that of the GFP control and are depicted as relative percentages of infection ± SD. (B) The experiment was performed as described for panel A, but cells were infected with SFV or SV40 for 6 h or 24 h, respectively. Infection by SFV or SV40 was analyzed by antibody staining against glycoproteins or T-antigen, respectively, using flow cytometry. The amounts of infection (±SD) relative to that in control-transfected cells are given. (C, D) HeLa or HaCaT cells were transfected with siRNA targeted against dynamin-2 or control for 48 h. siRNA-transfected HeLa or HaCaT cells were infected 48 h posttransfection with HPV PsVs as indicated. At 24 h p.i., luciferase activities were determined. The luciferase activities were normalized to LDH activities (relative to that in control-transfected cells; shown [±SD] in panel E) for cell viability and to the luciferase activity in control siRNA-transfected cells and are depicted as relative percentages of infection ± SD. (E) Cell lysates were analyzed for the levels of dynamin-2 or, as a loading control, α-tubulin by Western blotting.

entry. Therefore, HeLa and HaCaT cells were transfected with CD151-specific siRNA or a control siRNA for 48 h and subsequently infected (Fig. 5D and E). The efficiency of CD151 siRNA knockdown was controlled by Western blotting using a rabbit antiserum against CD151 (Fig. 5F) (11). RNAi-mediated knockdown of CD151 led to significant inhibition of HPV18, -16, and -31 infection (Fig. 5D and E). These data lead to the conclusion that tetraspanin-enriched microdomains may represent a common entry platform for all high-risk HPV types tested.

Since we observed that HPV16, -18, and -31 required similar host cell factors for entry, we analyzed whether the viruses would be commonly internalized and routed to the same endocytic target organelle. Previous work showed that, after uptake, HPV16 and HPV31 localize to late endosomal/lysosomal compartments, which are marked by the presence of LAMP-1 (9, 34). For analysis, PsVs of the three subtypes were covalently labeled with Alexa Fluor dyes, a procedure that does not affect the infectivity of particles (39). HeLa cells were simultaneously infected with HPV18, -16, and -31 and were fixed at 6 or 8 h p.i. The cells were stained with Hoechst stain to visualize the nuclei, and the degree of colocalization was determined by confocal microscopy and computational image analysis using Imaris (version 7.4.2; Bitplane). To assess the maximal degree of colocalization, the cells were also infected with two preparations of HPV16 that were labeled with different dyes. To determine the degree of coincidental colocalization, the cells were infected with HPV16 labeled with Alexa Fluor 647 (AF-647) for 6 h, after which the cells were superinfected with

HPV16 labeled with AF-488 for an additional 2 h. The AF-647-labeled virus marked partially internalized viruses, whereas the AF-488-labeled virus localized mostly to the surface of the cells (9).

At 6 or 8 h p.i., the viruses localized mostly to the perinuclear area (Fig. 6A to C; also data not shown). The degree of colocalization of HPV18/HPV16 or of HPV31/HPV16 was the same as for the control for maximal colocalization (HPV16/HPV16) at 6 h p.i. (Fig. 6B to D) or at 8 h p.i. (not shown), which indicated that HPV16, -18, and -31 are routed into the same compartment after internalization. As previously observed, HPV16 localized to LAMP-1-positive compartments in HPV16-infected cells, which indicated internalization into late endosomal/lysosomal compartments (Fig. 6D and E). In conclusion, internalization and intracellular transport of HPV18, -16, and -31 commonly routed the virions to late endosomes/lysosomes. Since the degree of colocalization at a given time after internalization appeared to be indistinguishable between the different HPV types, we concluded in addition that the viruses were internalized with similar kinetics, in line with our observation that all three viruses had identical infection kinetics.

The results from this study indicate that the high-risk-types HPV16, -18, and -31 share similar requirements for endocytic entry into host cells. Entry occurred over a protracted period of time that was indistinguishable between HPV16, -18, and -31. HPV entry was independent of clathrin, caveolin, dynamin, and lipid rafts but required actin polymerization dynamics. In addition, fluorescently labeled HPV particles were commonly inter-
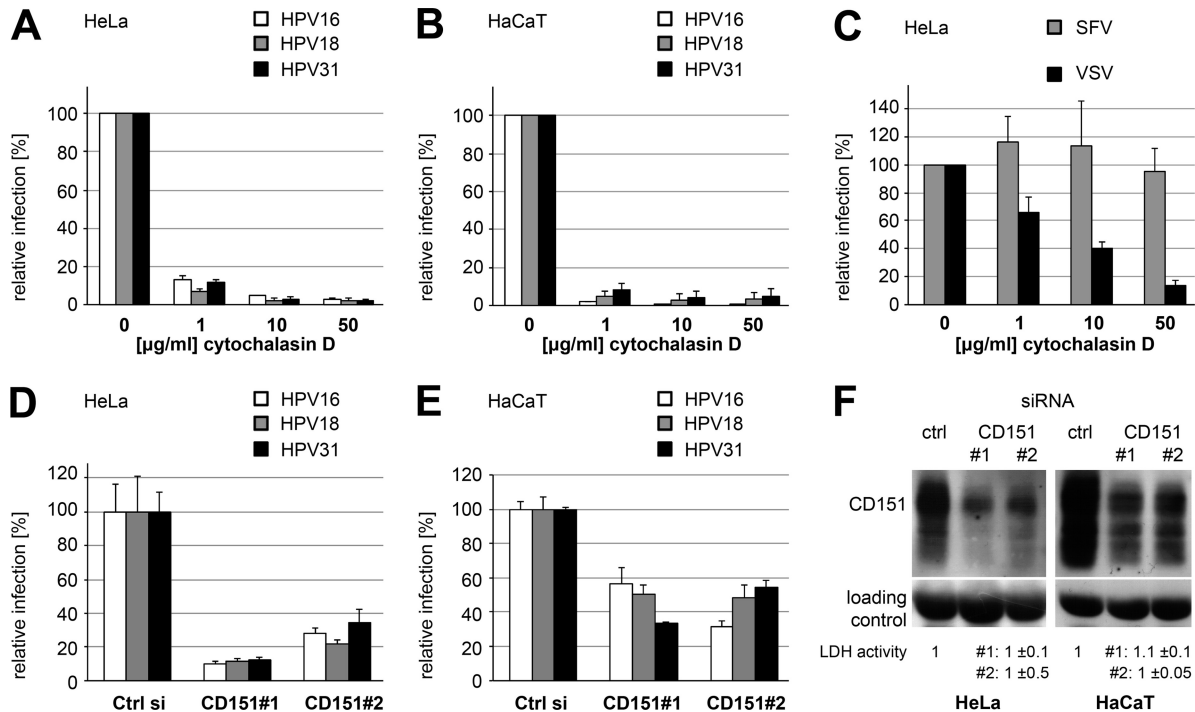
FIG 5 HPV infection commonly requires actin polymerization dynamics and the tetraspanin CD151. (A, B) HeLa or HaCaT cells were preincubated for 30 min with the indicated concentrations of cytochalasin D and subsequently infected with HPV PsVs. At 24 h p.i., luciferase activities were determined. Luciferase activities were normalized to LDH activities (relative to that in control-transfected cells; shown [±SD] in panel F) for cell viability and are depicted as percentages of infection ± SD relative to luciferase activity in DMSO-treated cells. (C) The experiment was performed as described for panel B, but cells were infected with SFV or VSV for 6 h. Infection by SFV or VSV was analyzed by antibody staining or GFP expression, respectively, using flow cytometry. The amounts of infection (±SD) relative to that in control siRNA-transfected cells are given. (D, E) HeLa or HaCaT cells were transfected with siRNA targeted against CD151 or control for 48 h. At 24 h p.i. with HPV PsVs, luciferase activities were determined. Luciferase activities were normalized to LDH activities (see panel F) for cell viability and to luciferase activity in control siRNA-transfected cells and are depicted as relative percentages of infection ± SD. (F) The experiment was performed as described for panels D and E, but 48 h after siRNA transfection, the levels of CD151 in HeLa and HaCaT cell lysates were analyzed by Western blotting with a rabbit anti-CD151 serum. SDS-PAGE was performed under nonreducing conditions. A nonspecific band recognized by the CD151 antibody is shown as a loading control.

nalized and routed to late endosomal/lysosomal compartments. Importantly, depletion of the tetraspanin CD151 reduced infection by all HPV types tested, suggesting that tetraspanin-enriched microdomains may provide a common entry platform for HPV16, -18, and -31. Overall, these findings suggested that HPV16, -18, and -31 make use of a similar mechanism of entry.

In agreement with previous reports (9, 10), HPV16 entry was insensitive to clathrin, caveolin, and dynamin depletion, to perturbation by DN mutants of CME or of dynamin-mediated processes, and to pharmacological perturbation of lipid rafts. Also, HPV16 entry was sensitive to drugs perturbing actin polymerization dynamics, which has been attributed to endocytic vesicle scission from the plasma membrane (9). Since no differences in the cellular requirements were observed for HPV18 infection, endocytosis of this HPV type likely occurred by a similar mechanism, which constitutes a potentially novel ligand-induced endocytic mechanism related to macropinocytosis (9). The hypothesis that all three HPV types make use of a similar mechanism is further strengthened by the fact that endocytosis and intracellular trafficking routed HPV16, -18, and -31 to the same subcellular LAMP-1-positive compartment, which has been defined to be the infectious route for HPV16 (9, 34) and to which HPV31 has been localized (34). In addition, our studies confirmed that HPV31 entry does not require a clathrin-mediated mechanism, as previously suggested (5, 12).

Interestingly, our results for HPV31 differed in part from previous observations with regard to the involvement of caveolin and dynamin and the sensitivity to cholesterol-depleting drugs. In one study, HPV31 infection of raft-derived particles appeared to be sensitive to nystatin treatment in human keratinocytes, whereas for PsV in COS-7 or 293TT cells, it was not (5, 12). In addition, Smith and colleagues (12) suggested that HPV31 entry uses caveolar endocytosis, based on the sensitivity of HPV31 infection to the expression of GFP-caveolin. In general, cellular perturbations bear the risk of pleiotrophic effects. To exclude such effects, perturbations have to be controlled rather rigorously. Therefore, infection studies of viruses with established entry requirements were used in this study as controls for the efficacy and specificity of perturbation. Virus infection was used as the control rather than uptake of certain cell biological ligands of specific endocytic pathways as this readout provides comparable sensitivities to perturbation. Hence, we surmise that our approach, using cell biological controls for the efficacy and specificity of perturbations, was in this respect superior to previous studies and that it provided a more realistic view of the cellular requirements of HPV31 than the studies without any such controls. When we used caveolin-1 knockdown, caveolin-1 knockout cells, and cholesterol depletion, HPV31 infection was unperturbed, whereas SV40 and SFV infections were blocked by cholesterol depletion. Our data thus support the notion that HPV31 entry would not occur via the caveolar
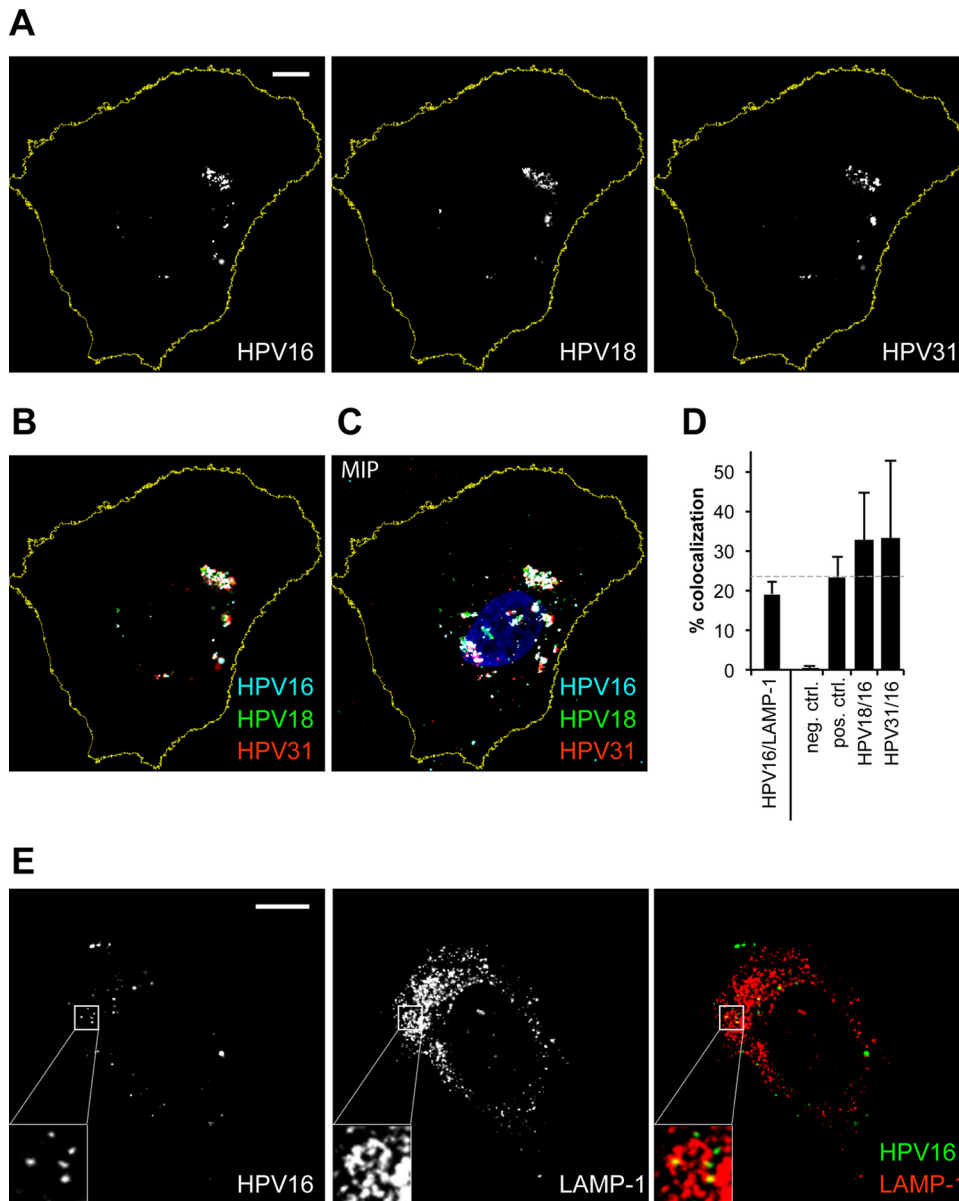
FIG 6 HPV16, -18, and -31 are commonly internalized into the same late endosomal/lysosomal compartments. HeLa cells were infected at the same time with HPV16, -18, and -31 PsVs labeled with AF-647, AF-488, and AF-594, respectively. Cells were fixed at 6 h p.i., stained with Hoechst stain for cell nuclei, and analyzed by laser scanning confocal microscopy using a Zeiss 510 Meta. (A, B) Depicted is a medial single focal plane of a representative cell showing the cell-associated fluorescent signals of HPV16, -18, or -31 (A) or the merge of signals (B). (B) Colocalization of the HPV18 (green), HPV31 (red), and HPV16 (cyan) signals is indicated by white. The outline of the cell is shown in yellow. (C) Maximum intensity projection (MIP) of the same cell, with the nucleus shown in blue and the cell outline in yellow. (D) Colocalization analysis was carried out by pixel-by-pixel analysis and thresholding using Imaris (Bitplane). Depicted are the relative amounts of colocalization of the signals. For the negative control (neg. ctrl.), cells were infected for different times with HPV16 (8 h) and HPV18 or -31 (2 h) to determine the amount of coincidental colocalization. For the positive control (pos. ctrl.), cells were infected simultaneously with HPV16 labeled with AF-488 and with HPV16 labeled with AF-594 to determine the amount of maximal colocalization. Shown are the mean values of three independent experiments ± SD. For each experiment, a minimum of 10 cells were analyzed. (E) HeLa cells were infected with HPV16 labeled with AF-488. Cells were fixed at 6 h p.i. and stained for LAMP-1 (mouse monoclonal antibody sc-20011 [Santa Cruz] and secondary anti-mouse AF-594 antibody [Invitrogen]) and analyzed as described above. Depicted is a medial single focal plane of a representative cell. Scale bars indicate 10 μm.

route, as caveola function clearly depends on the presence of cholesterol (40). Since the overexpression of caveolin-1 leads to the formation of modified late endosomes (previously termed "caveosomes" [33]), the sensitivity of HPV31 infection to GFP-caveolin overexpression may thus be caused by intracellular trafficking defects.

Similar to HPV31 entry, HPV16 entry has been attributed to different endocytic pathways, including pathways involving clathrin and caveolin (5–8). Although no study has directly addressed why a number of studies differed in their results on the requirements and localization of the virus, different production methods for HPV particles, the use of different cell types, and most impor-

tantly, pleiotrophic effects of inhibition have been suggested (8, 9, 41, 42). Here, HPV16, -18, and -31 particles were produced by the same methodology. The same number of viral particles was used for infection of the same keratinocyte-derived cells by the different HPV types. Under these conditions, the viruses showed the same requirements for the diagnostic determinants of the key endocytic pathways, which suggested that their mode of entry is similar as long as the viral particles enter with similar efficacy. A comprehensive future study may be warranted that elucidates whether and, if so, why virus particles produced by different methods show different requirements for entry. Conceivably, any interpretation of experimental results on the mode of uptake, trafficking, penetration, or nuclear import is made more difficult by impurities associated with viral particle preparations and a high viral load. The latter may be influenced by, among other factors, the stoichiometric ratio of genome equivalents or L2 incorporation into particles and/or how particles mature (43–45).

It is interesting to note that RNAi-mediated depletion of the tetraspanin CD151 reduced infection by HPV16, -18, and -31. In general, tetraspanins are part of specialized membrane microdomains associated with various cellular functions, including the regulation of cellular responses to external stimuli which control adhesion, motility, and proliferation (46–49). Tetraspanins were identified as an entry platform for HPV16 (10), and the role of tetraspanin microdomains in HPV16 infection has been suggested to include a function as a receptor/coreceptor or membrane-organizing structure for receptors and/or endocytic machinery (11). Based on the results of this study, their function may extend to HPV18 and -31.

In summary, the results of this study provide a framework upon which further comparative entry studies between different HPV types should be based. On the one hand, it would be interesting to comparatively analyze different virion particle preparations of the same HPV type for their mode of entry, whereas on the other hand, a more-detailed analysis on the cellular requirements for virus entry is required to more firmly attribute entry of the different HPV types to the same mechanism of endocytosis and intracellular trafficking. Indeed, it is conceivable that a more-detailed analysis will show more similarities but also highlight certain differences between HPV types that may already be reflected in the divergent findings in the literature.

ACKNOWLEDGMENTS

REFERENCES

1. **Longworth MS, Laimins LA.** 2004. Pathogenesis of human papillomaviruses in differentiating epithelia. Microbiol. Mol. Biol. Rev. **68**:362–372.
2. **Schelhaas M.** 2010. Come in and take your coat off—how host cells provide endocytosis for virus entry. Cell Microbiol. **12**:1378–1388.
3. **Mercer J, Schelhaas M, Helenius A.** 2010. Virus entry by endocytosis. Annu. Rev. Biochem. **79**:803–833.
4. **Doherty GJ, McMahon HT.** 2009. Mechanisms of endocytosis. Annu. Rev. Biochem. **78**:857–902.
5. **Hindmarsh PL, Laimins LA.** 2007. Mechanisms regulating expression of the HPV 31 L1 and L2 capsid proteins and pseudovirion entry. Virol. J. **4**:19. doi:10.1186/1743-422X-4-19.
6. **Day PM, Lowy DR, Schiller JT.** 2003. Papillomaviruses infect cells via a clathrin-dependent pathway. Virology **307**:1–11.
7. **Bousarghin L, Touze A, Sizaret PY, Coursaget P.** 2003. Human papillomavirus types 16, 31, and 58 use different endocytosis pathways to enter cells. J. Virol. **77**:3846–3850.
8. **Laniosz V, Dabydeen SA, Havens MA, Meneses PI.** 2009. Human papillomavirus type 16 infection of human keratinocytes requires clathrin and caveolin-1 and is brefeldin A sensitive. J. Virol. **83**:8221–8232.
9. **Schelhaas M, Shah B, Holzer M, Blattmann P, Kuhling L, Day PM, Schiller JT, Helenius A.** 2012. Entry of human papillomavirus type 16 by actin-dependent, clathrin- and lipid raft-independent endocytosis. PLoS Pathog. **8**:e1002657. doi:10.1371/journal.ppat.1002657.
10. **Spoden G, Freitag K, Husmann M, Boller K, Sapp M, Lambert C, Florin L.** 2008. Clathrin- and caveolin-independent entry of human papillomavirus type 16—involvement of tetraspanin-enriched microdomains (TEMs). PLoS One **3**:e3313. doi:10.1371/journal.pone.0003313.
11. **Scheffer KD, Gawlitza A, Spoden GA, Zhang XA, Lambert C, Berditchevski F, Florin L.** 2013. Tetraspanin CD151 mediates papillomavirus type 16 endocytosis. J. Virol. **87**:3435–3446.
12. **Smith JL, Campos SK, Ozbun MA.** 2007. Human papillomavirus type 31 uses a caveolin 1- and dynamin 2-mediated entry pathway for infection of human keratinocytes. J. Virol. **81**:9922–9931.
13. **Buck CB, Pastrana DV, Lowy DR, Schiller JT.** 2005. Generation of HPV pseudovirions using transfection and their use in neutralization assays. Methods Mol. Med. **119**:445–462.
14. **Buck CB, Pastrana DV, Lowy DR, Schiller JT.** 2004. Efficient intracellular assembly of papillomaviral vectors. J. Virol. **78**:751–757.
15. **Spoden GA, Besold K, Krauter S, Plachter B, Hanik N, Kilbinger AF, Lambert C, Florin L.** 2012. Polyethylenimine is a strong inhibitor of human papillomavirus and cytomegalovirus infection. Antimicrob. Agents Chemother. **56**:75–82.
16. **Knappe M, Bodevin S, Selinka HC, Spillmann D, Streeck RE, Chen XS, Lindahl U, Sapp M.** 2007. Surface-exposed amino acid residues of HPV16 L1 protein mediating interaction with cell surface heparan sulfate. J. Biol. Chem. **282**:27913–27922.
17. **Volpers C, Sapp M, Snijders PJ, Walboomers JM, Streeck RE.** 1995. Conformational and linear epitopes on virus-like particles of human papillomavirus type 33 identified by monoclonal antibodies to the minor capsid protein L2. J. Gen. Virol. **76**(Pt 11):2661–2667.
18. **Volpers C, Sapp M, Komly CA, Richalet-Secordel P, Streeck RE.** 1993. Development of type-specific and cross-reactive serological probes for the minor capsid protein of human papillomavirus type 33. J. Virol. **67**:1927–1935.
19. **Sapp M, Kraus U, Volpers C, Snijders PJ, Walboomers JM, Streeck RE.** 1994. Analysis of type-restricted and cross-reactive epitopes on virus-like particles of human papillomavirus type 33 and in infected tissues using monoclonal antibodies to the major capsid protein. J. Gen. Virol. **75**(Pt 12):3375–3383.
20. **Culp TD, Christensen ND.** 2004. Kinetics of in vitro adsorption and entry of papillomavirus virions. Virology **319**:152–161.
21. **Selinka HC, Giroglou T, Sapp M.** 2002. Analysis of the infectious entry pathway of human papillomavirus type 33 pseudovirions. Virology **299**:279–287.
22. **Selinka HC, Florin L, Patel HD, Freitag K, Schmidtke M, Makarov VA, Sapp M.** 2007. Inhibition of transfer to secondary receptors by heparan sulfate-binding drug or antibody induces noninfectious uptake of human papillomavirus. J. Virol. **81**:10970–10980.
23. **Schneider MA, Spoden GA, Florin L, Lambert C.** 2011. Identification of the dynein light chains required for human papillomavirus infection. Cell Microbiol. **13**:32–46.
24. **Wang LH, Rothberg KG, Anderson RG.** 1993. Mis-assembly of clathrin lattices on endosomes reveals a regulatory switch for coated pit formation. J. Cell Biol. **123**:1107–1117.
25. **Elferink JG.** 1979. Chlorpromazine inhibits phagocytosis and exocytosis in rabbit polymorphonuclear leukocytes. Biochem. Pharmacol. **28**:965–968.
26. **Watanabe S, Hirose M, Miyazaki A, Tomono M, Takeuchi M, Kitamura T, Namihisa T.** 1988. Calmodulin antagonists inhibit the phagocytic activity of cultured Kupffer cells. Lab. Invest. **59**:214–218.
27. **Amyere M, Payrastre B, Krause U, Van Der Smissen P, Veithen A, Courtoy PJ.** 2000. Constitutive macropinocytosis in oncogene-

transformed fibroblasts depends on sequential permanent activation of phosphoinositide 3-kinase and phospholipase C. Mol. Biol. Cell **11**:3453–3467.

28. **Giocondi MC, Mamdouh Z, Le Grimellec C.** 1995. Benzyl alcohol differently affects fluid phase endocytosis and exocytosis in renal epithelial cells. Biochim. Biophys. Acta **1234**:197–202.

29. **Benmerah A, Lamaze C, Begue B, Schmid SL, Dautry-Varsat A, Cerf-Bensussan N.** 1998. AP-2/Eps15 interaction is required for receptor-mediated endocytosis. J. Cell Biol. **140**:1055–1062.

30. **Marsh M, Helenius A.** 1980. Adsorptive endocytosis of Semliki Forest virus. J. Mol. Biol. **142**:439–454.

31. **Schlegel R, Willingham MC, Pastan IH.** 1982. Saturable binding sites for vesicular stomatitis virus on the surface of Vero cells. J. Virol. **43**:871–875.

32. **Damm EM, Pelkmans L, Kartenbeck J, Mezzacasa A, Kurzchalia T, Helenius A.** 2005. Clathrin- and caveolin-1-independent endocytosis: entry of simian virus 40 into cells devoid of caveolae. J. Cell Biol. **168**:477–488.

33. **Hayer A, Stoeber M, Ritz D, Engel S, Meyer HH, Helenius A.** 2010. Caveolin-1 is ubiquitinated and targeted to intralumenal vesicles in endolysosomes for degradation. J. Cell Biol. **191**:615–629.

34. **Smith JL, Campos SK, Wandinger-Ness A, Ozbun MA.** 2008. Caveolin-1-dependent infectious entry of human papillomavirus type 31 in human keratinocytes proceeds to the endosomal pathway for pH-dependent uncoating. J. Virol. **82**:9505–9512.

35. **Sieczkarski SB, Whittaker GR.** 2002. Dissecting virus entry via endocytosis. J. Gen. Virol. **83**:1535–1545.

36. **Marsh M, Bolzau E, Helenius A.** 1983. Penetration of Semliki Forest virus from acidic prelysosomal vacuoles. Cell **32**:931–940.

37. **Loerke D, Mettlen M, Yarar D, Jaqaman K, Jaqaman H, Danuser G, Schmid SL.** 2009. Cargo and dynamin regulate clathrin-coated pit maturation. PLoS Biol. **7**:e57. doi:10.1371/journal.pbio.1000057.

38. **Cureton DK, Massol RH, Saffarian S, Kirchhausen TL, Whelan SP.** 2009. Vesicular stomatitis virus enters cells through vesicles incompletely coated with clathrin that depend upon actin for internalization. PLoS Pathog. **5**:e1000394. doi:10.1371/journal.ppat.1000394.

39. **Schelhaas M, Ewers H, Rajamaki ML, Day PM, Schiller JT, Helenius A.** 2008. Human papillomavirus type 16 entry: retrograde cell surface transport along actin-rich protrusions. PLoS Pathog. **4**:e1000148. doi:10.1371/journal.ppat.1000148.

40. **Pelkmans L, Helenius A.** 2002. Endocytosis via caveolae. Traffic **3**:311–320.

41. **Schiller JT, Day PM, Kines RC.** 2010. Current understanding of the mechanism of HPV infection. Gynecol. Oncol. **118**:S12–S17.

42. **Florin L, Sapp M, Spoden GA.** 2012. Host-cell factors involved in papillomavirus entry. Med. Microbiol. Immunol. **201**:437–448.

43. **Fligge C, Schafer F, Selinka HC, Sapp C, Sapp M.** 2001. DNA-induced structural changes in the papillomavirus capsid. J. Virol. **75**:7727–7731.

44. **Buck CB, Thompson CD, Pang YY, Lowy DR, Schiller JT.** 2005. Maturation of papillomavirus capsids. J. Virol. **79**:2839–2846.

45. **Buck CB, Cheng N, Thompson CD, Lowy DR, Steven AC, Schiller JT, Trus BL.** 2008. Arrangement of L2 within the papillomavirus capsid. J. Virol. **82**:5190–5197.

46. **Boucheix C, Rubinstein E.** 2001. Tetraspanins. Cell. Mol. Life Sci. **58**:1189–1205.

47. **Yunta M, Lazo PA.** 2003. Tetraspanin proteins as organisers of membrane microdomains and signalling complexes. Cell Signal. **15**:559–564.

48. **Hemler ME.** 2001. Specific tetraspanin functions. J. Cell Biol. **155**:1103–1107.

49. **Yanez-Mo M, Barreiro O, Gordon-Alonso M, Sala-Valdes M, Sanchez-Madrid F.** 2009. Tetraspanin-enriched microdomains: a functional unit in cell plasma membranes. Trends Cell Biol. **19**:434–446.